

## **ACTION OF HIGH-ENERGY NEODYMIUM LASER RADIATION PULSES HAVING A DIFFERENT SPACE-TIME SHAPE ON METALS**

**V. K. Goncharov**

UDC 621.373.826:533.9

*The role of different factors favorable for the arrival of the liquid-drop phase of the target material at the erosion flame has been elucidated. The crushing of particles of the liquid-drop phase in the process of their motion toward the laser beam has been revealed. The conditions under which the liquid-drop phase influences a laser-radiation loss have been determined. The methods of control of the parameters of the liquid-drop phase in erosion plasma flames have been found.*

As is known, in the case of action of laser radiation of moderate power density ( $10^5$ – $10^8$  W/cm<sup>2</sup>) on metals, the erosion products consist of a vapor, a plasma, and particles of the condensed phase of the target material [1]. Initially, smaller particles of the liquid-drop phase, which are formed due to volumetric vaporization, arrive at the erosion flame. By the end of the laser pulse, larger particles formed through the hydrodynamic mechanism appear in the erosion products. Particles moving toward the laser beam scatter and absorb its energy. However, in all the experiments [1], different metals were exposed to the radiation of a pulsed neodymium laser operating in the free-running mode. This lasing mode is characterized by the fact that a radiation pulse consists of individual "spikes" of duration 1–3 μsec, which are separated by 1–6-μsec intervals. These spikes are distributed rather randomly in the time of appearance and amplitude over the cross section of the beam. Clearly, this space-time nonuniformity of laser radiation makes the interpretation of experimental results difficult. More accurate measurements are possible with laser pulses having a smooth shape.

To perform experiments on the action of laser radiation of power density  $10^5$ – $10^8$  W/cm<sup>2</sup> on metals, it is often necessary to irradiate laser targets in large spots; therefore, the energy of the laser pulses must be fairly high. For this purpose, we designed a facility based on neodymium-doped glasses, which included a master oscillator and several amplifiers. The general scheme of the experiment is shown in Fig. 1. A standard GOS-1001M head with a confocal cavity was used as the master oscillator. The working body 6 of neodymium-doped glass of the type GLS-6 has a length of 618 mm and a diameter of 30 mm. It was chosen from the viewpoint of provision of the maximum pumping of the working medium with the use of standard IFP-20000 illuminating lamps. The cavity formed by spherical mirrors with a radius of curvature of 2.5 m (totally reflecting mirror 5 and semireflecting mirror 7) has a large positive feedback (the reflectance of the semireflecting mirror is ~70%).

Using a high intensity of the pumping-radiation energy, a large positive feedback in the cavity, and a negative feedback that is due to a change in the concentration of particles at the metastable level, it has been possible to realize a quasistationary lasing mode [2]. In this mode, one can obtain a fairly smooth radiation pulse, exclusive of the leading edge. Because of the transient processes, fairly intense oscillation processes occur, as a rule, at the leading edge of a radiation pulse. A radiation pulse with uniform characteristics was

---

A. N. Sevchenko Scientific-Research Institute of Applied Physical Problems, Belarusian State University, Minsk, Belarus. Translated from *Inzhenerno-Fizicheskii Zhurnal*, Vol. 74, No. 5, pp. 87–97, September–October, 2001. Original article submitted July 17, 2000; revision submitted February 27, 2001.

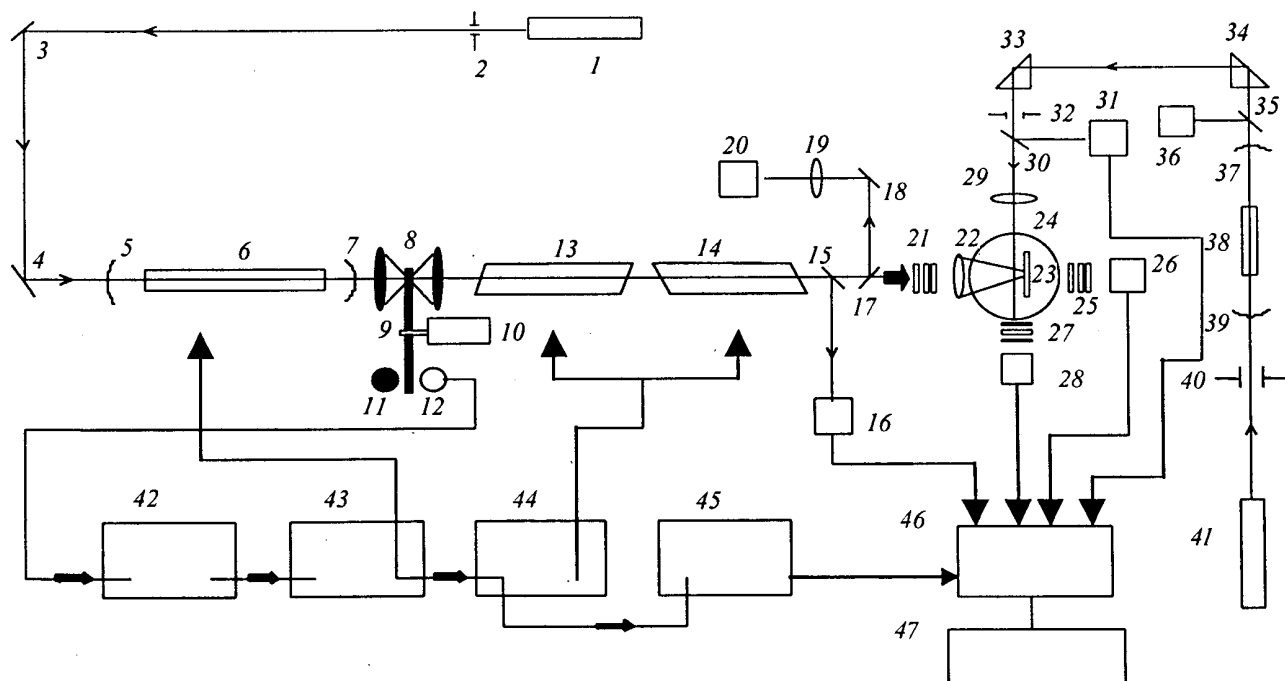


Fig. 1. General scheme of the experiment: 1, 41) alignment lasers; 2, 32, 40) diaphragms; 3, 4) rotating mirrors; 5, 7) spherical mirrors; 6) working body of the master oscillator; 8) system of two confocal lenses; 9) rotary diaphragm; 10) electric motor; 11) synchronizing lamp; 12) triggering photodiode; 13, 14) amplifiers; 15, 17, 18, 30, 35) rotating plates; 19, 22, 29) lenses; 16, 28, 31) photodiodes; 20, 36) calorimeters; 21, 25, 27) light filters; 23) target; 24) integrating sphere; 26) photomultiplier; 33, 34) rotating prisms; 37-39) ruby laser; 42-45) pulse generators; 46) multichannel automated recorder; 47) computer.

obtained using a mechanical shutter that cut the initial and the end nonstationary parts of the quasistationary pulse. As such, we used a system of confocal lenses 8 in the common focus of which a rotary metallic disk 9 with a slot was positioned. On the one hand, such a system allows one to make the edges of the cut radiation pulse steeper, and on the other hand, it isolates the oscillator from the optical radiation reflected from the object under study. On the modulator disk there is a hole between the incandescent lamp 11 and the photodiode 12, which is meant for the formation of an electric signal that is transformed using delayed-pulse generators 42-45 into pulses of triggering and synchronization of the devices involved in the experiment.

As a result, it has been possible to obtain a radiation pulse of duration 50-500  $\mu\text{sec}$ , which has a nearly rectangular shape with a fairly uniform flat top. The temporal shape of such a pulse is shown in Fig. 2a (1). Its energy must be fairly high; this being so, several amplifiers 13 and 14 are used after the oscillator (see Fig. 1) — standard GOS-1001M heads with working bodies of diameter 45mm and length 618 mm. To prevent undesirable feedback from the master oscillator, the ends of these working bodies were cut at an angle of  $85^\circ$  to the optical axis. Since the radiation pulse of the master oscillator has a rather high energy ( $\sim 100$  J), its amplification without special precautions distorts the temporal shape of the pulse because of a decrease with time in the concentration of particles at the metastable level of the working medium of the amplifier. The temporal shape of such a pulse is shown in Fig. 2a (2). Using the delay in the start of the amplifier relative to the master oscillator, one can find such a moment when the nonstationarity of the gain factor owing to an increase in the pumping intensity compensates for its decrease owing to the depletion of the metastable level. In this case, it has been possible to obtain an amplified radiation pulse with minimum

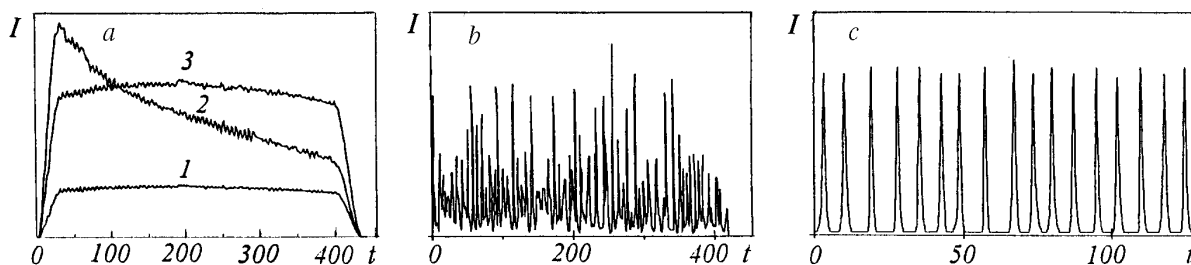


Fig. 2. Temporal shape of laser pulses: a) neodymium laser [1) master oscillator with a confocal cavity; 2) amplified pulse without a delay; 3) the same with a delay]; b) neodymium laser operating in the free-running mode; c) ruby laser operating in the regular lasing mode.  $I$ , rel. units;  $t$ ,  $\mu\text{sec}$ .

distortions (see Fig. 2a (3)). As is known [3], in the case of generation of a quasistationary pulse by a generator with a confocal cavity, because of the high multimode property of the radiation with a sufficient uniformity in time, the laser beam has a good spatial uniformity. On the above-described facility it has been possible to obtain at best rectangular radiation pulses with an energy of up to 500 J and a space-time nonuniformity of no worse than 3%.

The erosion laser flame formed by the action of laser radiation of moderate power density on metals represents in essence a two-phase flow consisting of drops and a plasma. One method that allows one to control the size of the condensed particles in plasma flows in the real time of their existence is laser probing. By the ratio between the scattered and absorbed components of the probing radiation one can judge the size of the particles of the liquid-drop phase. However, to do this it is necessary to divide the total loss of the probing laser radiation into the loss by scattering and the loss by absorption. For this purpose, the laser target 23 (see Fig. 1) was positioned in the photometric sphere 24. As the probing radiation, the radiation of a ruby laser 37–39 was used. In the experiment, we controlled simultaneously the power density of the probing radiation incident perpendicularly to the axis of the erosion flame using the photodetector 31, the power density of the radiation transmitted by the erosion flame (photodetector 28), and the power density of the ruby-laser radiation scattered by the erosion flame (photodetector 26). The coefficients of scattering and absorption of probing radiation by the erosion laser can be found from the balance of the probing-radiation energy. Comparing the experimentally obtained ratio of the absorbed component of the probing radiation to the scattered component with the analogous ratio calculated according to the Love–Mie theory, one can determine the diameters of the particles of the liquid-drop phase. This method of control of the size of the condensed-phase particles in plasma flows in the real time of their existence is described in more detail in [4]. Experimentally determining the dimensions of the flame in the probing zone, one can also find the concentration of the particles [5]. Collection, storage, and processing of experimental data were automated using a multiparameter automated recorder 46 (see [6]) designed by us and a personal computer 47. The functions of the other elements of the general scheme of the experiment are listed in the caption to Fig. 1.

There is a theoretical work [7] in which the problem of the action of stationary laser radiation on metals with an ideal structure is considered. It has been shown that in this case, volume vaporization that is responsible for the formation of a finely dispersed liquid-drop phase cannot occur, because the liquid metal layer formed under these conditions is too thin.

In [8–10], different factors that can be favorable to the appearance of volume vaporization are discussed: space-time nonuniformity of laser radiation, gases dissolved in the metal, different impurities, and structural inhomogeneities.

To determine the degree of their influence on the volume vaporization, we have conducted experiments [11] in lead targets.

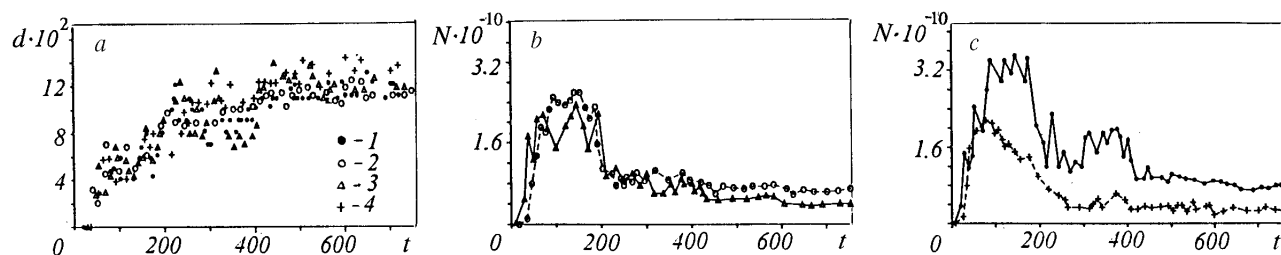


Fig. 3. Time variation of the size (a) and concentrations (b) of particles in the case of the action of a pulse with 100% modulation (1) and a smooth pulse (2) on a lead target remelted in air and in the case of the action of a pulse with 100% modulation (3) and a smooth pulse (4) on a lead target remelted in vacuum.  $t$ ,  $\mu\text{sec}$ ;  $d$ ,  $\mu\text{m}$ ;  $N$ ,  $\text{cm}^{-3}$ .

The targets were produced by remelting the lead: in air in one case and in vacuum in the other case with the aim of decreasing significantly the content of gases in the lead remelted in vacuum.

Furthermore, the action was carried out by different pulses of a neodymium laser. In one case, a rectangular pulse of duration 400–450  $\mu\text{sec}$  was cut by a mechanical shutter from the millisecond pulse of a laser operating in the free-running mode. Such a pulse had 100% amplitude modulation with spikes of microsecond duration with a rather random space-time distribution. In the other case, a smooth rectangular pulse was obtained using the mechanical shutter from the pulse of a neodymium laser with a confocal cavity. In such a variant, the pulse has a space-time nonuniformity no worse than 3%. The shapes of these pulses are shown in Fig. 2a and b. The probing ruby laser operated in the regular lasing mode (Fig. 2c) and had a power density of no more than  $10^4 \text{ W/cm}^2$  in the probing zone so as not to disturb the medium probed. The probing was carried out at a distance of 1.5 mm from the surface of the target perpendicularly to the axis of the erosion flame.

The experiments were conducted for a power density of the neodymium laser of  $6.5 \cdot 10^5 \text{ W/cm}^2$ . The diameter of the illuminated spot on the target was 0.9 cm. Under these experimental conditions, it has been possible to separate in space and time the liquid-drop-phase particles formed owing to volume vaporization and through the hydrodynamic mechanism. Results of the experiments are presented in Fig. 3.

It is seen from Fig. 3 that both the gas content in the target material and the space-time nonuniformity of the acting laser radiation influence only slightly the diameters of the target-material particles. They are determined by the thermophysical properties of lead. The increase in the particle size with time is apparently due to the increase in the thickness of the melt owing to heat conduction [12]. However, the concentration of particles depends strongly on experimental conditions. Their minimum amount is formed when a smooth laser pulse acts on a lead target remelted in vacuum. The maximum concentration of particles is observed in the case where a laser pulse with 100% modulation (see Fig. 3c) acts on a lead target remelted in air.

The concentration of particles formed as a result of the action of a smooth laser pulse on the lead remelted in air is fairly close to the concentration of particles formed as a result of the action of a modulated laser pulse on the lead remelted in vacuum, although, in the first case, the curve lies somewhat higher (see Fig. 3b).

Analysis of the results presented in Fig. 3b and c allows the conclusion that the space-time nonuniformity and the gases dissolved in the metal facilitate significantly the process of volume vaporization owing to which the finely dispersed liquid-drop phase is formed. The influence of these two factors is comparable.

In [9], where metals with a different content of gases were exposed to the radiation of a free-running neodymium laser, it has been shown that the gas content influences significantly the formation of the liquid-drop phase. In [10], it has been pointed out that in the case where metal targets are irradiated by a quasista-

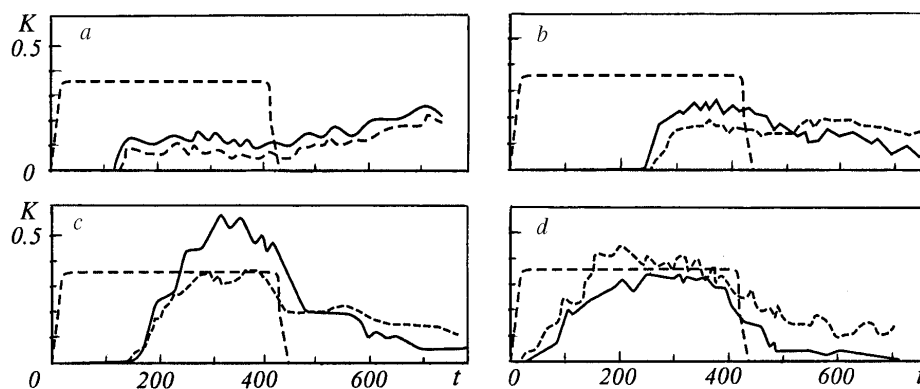


Fig. 4. Time variation of the absorption coefficient (solid lines) and the scattering coefficients (dashed lines) of probing radiation for targets of polycrystalline silicon (a), single-crystalline silicon (b, c), and single-crystalline silicon with an abrasive-material inclusion (d); a, b, d)  $q = 4.3 \cdot 10^6 \text{ W/cm}^2$ , c)  $6.8 \cdot 10^6 \text{ W/cm}^2$ . The rectangle shows the conditional shape of the active laser pulse.  $t$ ,  $\mu\text{sec}$ .

tionary laser pulse, the formation of the liquid-drop phase is dependent on both the gases dissolved in the metals and the space-time nonuniformity of laser radiation. It should be noted that under the conditions of these experiments, the liquid-drop phase of the target material is formed as a result of two processes simultaneously: the process of volume vaporization and the hydrodynamic process. The latter can turn out to be more significant. However, the results of the present work show that the role of the hydrodynamic mechanism in the formation of fairly large drops is minimum. In [8–10], it has been established that the volume vaporization on different inclusions and artificial centers is also of importance in the dynamics of disintegration of metals. In [1], experiments on the action of the pulsed radiation of a neodymium laser on molybdenum and copper targets produced by the method of powder metallurgy have been carried out. It has been shown that the inclusions of molybdenum grains in the copper act as artificial centers and facilitate the process of volume vaporization. However, noticeable results have been obtained when 20% of molybdenum was added to the copper. In real metals (except for exotic alloys and composite materials) the amount of such inclusions is rather low. Therefore, volume vaporization in these metals is facilitated mainly because of the gases contained in them and owing to the space-time nonuniformity of laser radiation as the strongest factors.

Should the experimental conditions be such that the above-described factors favorable to volume vaporization are absent or are reduced to a minimum, volume vaporization can be facilitated on inhomogeneities that are related to the polycrystalline structure of the metal (structural inhomogeneities). Of interest are comparative experiments on the action of laser radiation on a polycrystal of metal and a single crystal. However the author did not have single crystals of a metal at his disposal. Therefore, experiments were carried out with targets of high-purity polycrystalline and single-crystalline silicon. It is known [3] that, as a result of the action of a powerful laser radiation on semiconductor materials, they are metallized in times of  $10^{-10}$ – $10^{-9}$  sec and then act as metals.

The action was performed by a nearly rectangular pulse of the neodymium-laser radiation. The experiments were carried out at different power densities of the acting radiation, and they have shown that the disintegration of both the polycrystalline and the single-crystalline silicon begins for a power density of  $4 \cdot 10^5 \text{ W/cm}^2$ . In this case, the disintegration products are transparent to probing radiation, i.e., liquid drops are not formed. In the polycrystalline silicon, particles begin to appear in the erosion flame for an acting radiation power density of  $2.7 \cdot 10^6 \text{ W/cm}^2$  and in the single-crystalline silicon, they appear for  $4.2 \cdot 10^6 \text{ W/cm}^2$ . It has been established that the finely dispersed liquid-drop phase is formed more rapidly and intensely in the

single-crystalline silicon. This is easily seen from the time variation of the absorption and scattering coefficients of probing radiation (Fig. 4a and b) which have been obtained for the same power density ( $4.3 \cdot 10^6$  W/cm<sup>2</sup>) of the acting neodymium-laser radiation. In this case, the formation of the liquid-drop phase in the single-crystalline silicon target begins much later.

It may be suggested that the main factor that brings about the formation of the liquid-drop phase in the polysilicon is volume vaporization that is facilitated owing to structural inhomogeneities responsible for a local superheating. In the target of single-crystalline silicon, there are no such structural inhomogeneities; however, the liquid-drop phase arises, even though with a marked time delay, in this case, too. It can be formed because of the instability of the vaporization front [14–16] or owing to the explosion of a metastable liquid [16].

The behavior of the absorption and scattering coefficients in the case of probing of the erosion flame of the target, of single-crystalline silicon points to a more rapid and intense ejection of the liquid-drop phase, which makes the hypothesis of the explosion of a metastable liquid more attractive in this case. This is seen especially clearly when the power density of the acting laser radiation increases (Fig. 4c).

For comparison of the influence of different conditions of formation of the liquid-drop phase of a silicon target, we present results of experiments on the action of laser radiation on a target of single-crystalline silicon contaminated by relatively large particles of an abrasive material (Fig. 4d). In this case, it is seen that different inclusions influence more significantly the process of volume vaporization than structural inhomogeneities.

Thus, the investigations carried out allow the conclusion that for real metals, the formation of an erosion flame with a finely dispersed liquid-drop phase of the target material due to volume vaporization is facilitated first of all owing to gases dissolved in the metal and to the space-time nonuniformity of laser radiation. The action of these two factors is comparable. The next factor is the presence of different inclusions and artificial centers in the metal. In the absence of these three conditions, the process of volume vaporization is facilitated by structural inhomogeneities. Finally, in the absence of all these reasons, the formation of the liquid-drop phase, though difficult, is also realized for an increased power density. This can be both due to the instability of the vaporization front and owing to the explosion of the metastable liquid.

In the first experiments [1], to reveal liquid-drop particles of the target material in the erosion flame, which are formed owing to volume vaporization, the conditions and the metals were taken such that the process of volume vaporization is maximum. This is explained by the fact that the measuring devices used in these experiments were not automated and did not possess a high sensitivity. At a later time, an automated system of collection, storage, and processing of data was designed and the sensitivity of the scattering channel was significantly increased. Owing to this, it has been possible to perform experiments with a wide range of metals [1] and establish that volume vaporization is characteristic of all the investigated metals for certain power densities. Unfortunately, in these experiments, only the radiation of a free-running neodymium laser was used as the acting radiation.

The above-described experiments on the action of laser-radiation pulses with a different space-time structure on metal targets produced by different methods have shown that the formation of a finely dispersed liquid-drop phase of the target material owing to volume vaporization is a common phenomenon for metals. Different metals show only quantitative distinctions.

In all these experiments, the parameters were monitored at the same distance from the target surface (1.5 mm). To reveal changes in the parameters of the liquid-drop phase in the process of motion along the erosion flame, we performed probing at different distances  $h$  from the target surface under the same conditions of the action [17]. It should be noted that the investigations of the liquid-drop phase by the method of transverse laser probing near the surface meet with crucial difficulties, since a hollow is formed in the irradiated zone in the process of laser action and its edges shield the vaporizing surface. To eliminate the shielding of probing radiation, the targets were made in the form of cylinders whose diameter was comparable with

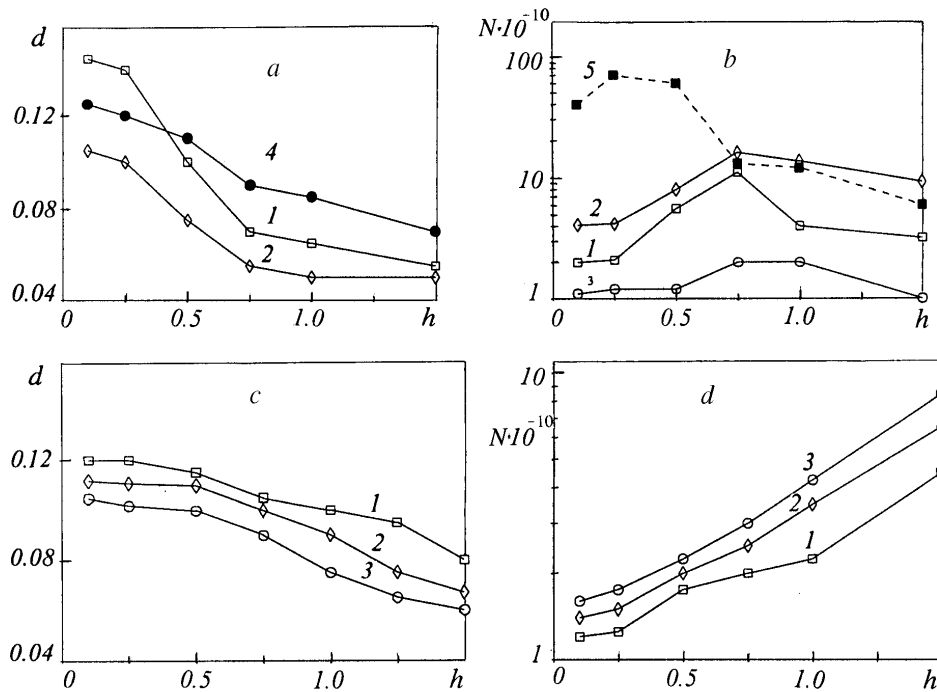


Fig. 5. Dependence of the diameter and concentration of particles on the distance from the surface of the lead (a, b) and nickel (c, d) targets at the instants of time  $t = 100$  (1), 200 (2), 300 (3), and 400  $\mu\text{sec}$  (4) for a power density of  $q = 2.4 \cdot 10^5 \text{ W/cm}^2$  [curves 1–4 (a, b)],  $q = 4.5 \cdot 10^5 \text{ W/cm}^2$  (curve 5), and  $q = 1.3 \cdot 10^6 \text{ W/cm}^2$  [curves 1–3 (c, d)].  $d$ ,  $\mu\text{m}$ ;  $N$ ,  $\text{cm}^{-3}$ ;  $h$ ,  $\text{mm}$ .

the diameter of the irradiation spot and the radiation acted on the end of the cylinder. In this case, a hollow is not formed and the target surface disintegrates uniformly, which makes it possible to carry out investigations at distances from the target surface of up to 0.1 mm.

As the acting (plasma-forming) radiation, we used the radiation of a neodymium laser that generated nearly rectangular pulses. The radiation was focused by a lens to a spot 0.9 cm in diameter on a target; the diameter of the target end was also 0.9 cm.

As a result of these experiments, we were able to determine changes in the size of the liquid-drop-phase particles and in their number concentration with distance from the target surface. Figure 5a and c shows the curves of variation of the size of the particles of lead and nickel targets for different instants of time for a power density of the acting neodymium-laser radiation of  $q = 2.4 \cdot 10^5 \text{ W/cm}^2$  (a) and  $q = 1.3 \cdot 10^6 \text{ W/cm}^2$  (c). It is seen that particles of maximum size are located near the target surface, while with distance from the surface the particle size decreases.

Figure 5b and d shows the behavior of the number concentrations of liquid-drop-phase particles for a lead target (b) and a nickel target (d) for different instants of time. For the power density of the neodymium-laser radiation acting on the lead  $q = 2.4 \cdot 10^5 \text{ W/cm}^2$  (b), the concentration of the particles increases with distance from the target surface up to 0.75 mm. As the distance increases further, the concentration of particles begins to decrease. Analysis of the curves (see Fig. 5) allows the suggestion that such behavior of the concentration of particles is related to the competition of two processes: increase in the number of particles owing to crushing and decrease in their number owing to complete vaporization.

As the power density of the neodymium-laser radiation acting on the lead target increases, the maximum of the particle concentration approaches the target surface (Fig. 5b, curve 5), which supports the sug-

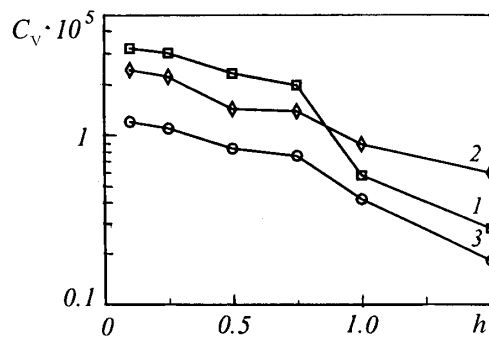


Fig. 6. Dependence of the volume concentration of liquid-drop-phase particles on the distance from the surface of the lead target for a power density of the neodymium laser of  $2.4 \cdot 10^5 \text{ W/cm}^2$  for a time of measuring after the beginning of the action of  $t = 100$  (1), 200 (2), and 400  $\mu\text{sec}$  (3).  $h$ , mm.

gestion made above. This means that for a higher power density of the acting radiation the process of crushing of particles in their motion along the flame begins earlier, and the concentration of the particles is much higher because of the change in the conditions in the surface layer of the target.

The number concentrations of particles of the nickel-target material act qualitatively in a similar manner. As the distance from the target surface increases, the concentration of particles increases up to 1.5 mm. Then it decreases, but the scattered component of the probing radiation of the ruby laser decreases significantly because of the decrease in the particle size and its recording becomes difficult under our conditions. As a consequence of this, sufficiently exact quantitative measurements of the concentration of the particles can be carried out only at an increased real sensitivity of the scattering channel of the measuring system. However, the qualitative behavior of the scattering and absorption coefficients of the probing radiation points to the fact that the size and concentrations of the particles decrease when the distance from the surface of the nickel target increases by more than 1.5 mm. Consequently, with a power density of the acting radiation of  $q = 1.3 \cdot 10^6 \text{ W/cm}^2$  (d), crushing of particles of the nickel target occurs at heights of the erosion flame of up to  $h = 1.5 \text{ mm}$ . The increase in the number concentration of the particles can occur not only owing to their crushing because of the heating, but also owing to the appearance of particles as a result of condensation [12]. To check this, we have measured the volume concentrations of the particles. Results of measurements for the lead target exposed to radiation with a power density of  $q = 2.4 \cdot 10^5 \text{ W/cm}^2$  are presented in Fig. 6. It is seen that when the distance from the target surface increases, the volume concentration decreases. This points to the fact that under the conditions of real experiments, of the competing processes of condensation and complete vaporization of particles, the latter is dominating. Consequently, the fact that the concentration of particles increases with distance from the target surface can be explained by their crushing in the process of motion owing to superheating.

Thus, the investigations carried out with targets of special shape made it possible to measure the space-time distribution of the size and concentrations of the target-material particles near the surface of the target by the method of transverse laser probing. It has been shown experimentally that there exist such conditions of the action of laser radiation on metals under which the concentration of particles of the finely dispersed liquid-drop phase, which enter the erosion flame from the target surface owing to volume vaporization, increases with distance from the target. In this case, the diameters of the particles decrease — they crush because of the superheating. On the other hand, particles are vaporized completely in the process of motion, owing to which their size and concentrations decrease. Because of the competition of the processes of crushing and vaporization of particles, a maximum of the particle concentration is observed at a certain



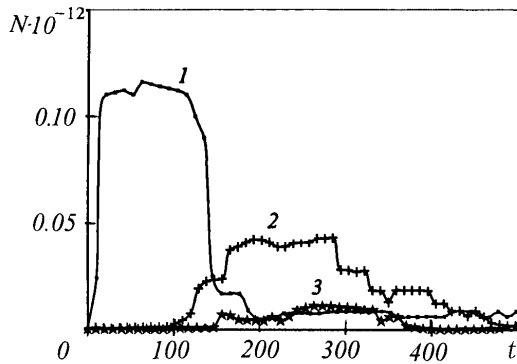


Fig. 7. Variation of the concentration of liquid drops of the lead target for a power density of  $4.6 \cdot 10^5$  (1),  $2.3 \cdot 10^5$  (2), and  $1.5 \cdot 10^5$   $\text{W/cm}^2$  (3).  $t$ ,  $\mu\text{sec}$ .

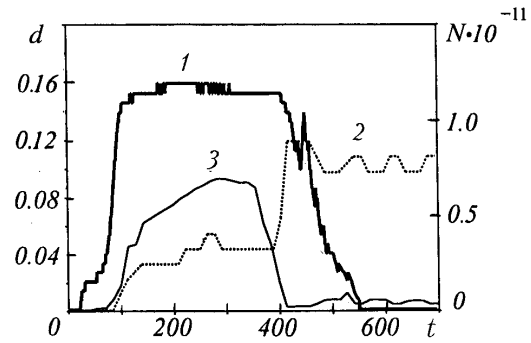


Fig. 8. Time variation of the luminescence intensity of an erosion laser flame in arbitrary units (1), of the size of particles (2), and of their concentrations (3).  $t$ ,  $\mu\text{sec}$ ;  $d$ ,  $\mu\text{m}$ ;  $N$ ,  $\text{cm}^{-3}$ .

distance from the target surface. The distance at which this occurs is determined by the target material and the power density of the acting radiation.

Because of the fact that in the experiments we were able to perform measurements at a distance of 0.1 mm from the vaporizing surface of the target, it became possible to carry out investigations on the beginning of formation of particles of the liquid-drop phase in the laser-erosion products, which are formed owing to volume vaporization. To do this, it is desirable that the sensitivity of the measuring devices be maximum in the process of monitoring of the concentration of particles. In this case, we were able to increase the minimum recorded number concentration of the particles (liquid drops) to  $10^8 \text{ cm}^{-3}$ .

In the work, we carried out investigations with erosion flames of targets of Zn, Sn, Pb, and Ni. The experiments have shown that beginning with a certain power density of the acting radiation, particles of the finely dispersed liquid-drop phase, which are formed owing to volume vaporization, enter the erosion flame practically immediately after the beginning of the action. In our case, the temporal resolution of measurements depends on the value of the interval between individual spikes of the probing ruby-laser radiation, which is  $\sim 10 \mu\text{sec}$ . Initially, the formation of particles owing to volume vaporization proceeds fairly intensely and the determination of the time presents no problems, while the accuracy is determined by a time of  $10 \mu\text{sec}$ .

Of the metals investigated, lead was found to be the lowest threshold for the formation of volume vaporization. For a power density of the acting neodymium-laser radiation of  $4.6 \cdot 10^5 \text{ W/cm}^2$ , volume vaporization appears practically immediately after the beginning of the action (Fig. 7). As the power density of the acting radiation decreases, volume vaporization appears with a delay whose value increases with decrease in the power density. It should be noted that the time zero of the abscissa axis in the figures corresponds to the beginning of lasing of the neodymium laser.

In recording the time of appearance of volume vaporization when its delay relative to the beginning of the action occurs, it is necessary to determine the time of appearance of a plasma. For this purpose, the plasma radiation in a wide spectral range was extracted from the zone under investigation using a quartz capillary and recorded using an FEU-68.

Using the lead target as an example, we can follow the dynamics of development of the erosion laser flame of metals. The experiments have shown that for each metal there are such conditions of laser action under which, after a certain time after the beginning of irradiation the disintegration products consist of a

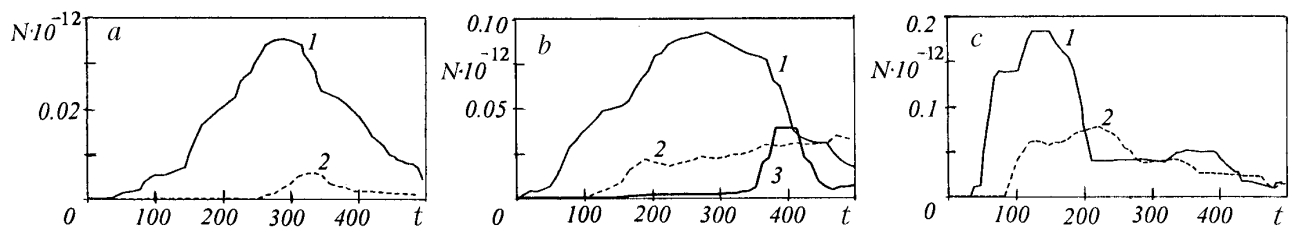


Fig. 9. Variation of the concentration of liquid drops with time for: a) nickel target for a power density of acting radiation of  $1.2 \cdot 10^6$  W/cm<sup>2</sup> (1),  $9 \cdot 10^5$  (2); b) zinc target for a power density of acting radiation of  $6.3 \cdot 10^5$  (1),  $5.2 \cdot 10^5$  (2),  $2.7 \cdot 10^5$  (3); c) tin target for a power density of acting radiation of  $7.7 \cdot 10^5$  W/cm<sup>2</sup> (1),  $4.6 \cdot 10^5$  (2).  $t$ ,  $\mu$ sec;  $N$ , cm<sup>-3</sup>.

luminous vapor practically transparent to radiation (Fig. 8, curve 1). After a time after the erosion flame is formed from this vapor, small liquid drops of the target material, which are formed owing to volume vaporization, begin to enter the flame. Approximately after 400  $\mu$ sec, larger particles that have much lower concentrations are formed in the flame through the hydrodynamic mechanism (Fig. 8, curves 2 and 3). For the remaining investigated metals, an analogous law is true, with the only difference that the power density of the acting neodymium-laser radiation for which this occurs is characteristic of each metal. This is easily seen from Fig. 9. Such behavior of the beginning of volume vaporization is explained by the dissimilar optical and thermophysical characteristics of the metals.

Thus, the experiments with a cylindrical target made it possible to carry out transverse laser probing near the surface and determine the beginning of volume vaporization in the laser metal targets by measuring the concentration of small liquid drops of the target material. Initially, the erosion flame consists of the transparent, in practice, luminous vapor of the target material. Then, owing to volume vaporization, small liquid drops enter the erosion flame with a time delay. The delay in the appearance of volume vaporization depends on the power density of the acting laser radiation and on the thermophysical characteristics of the target material. When the first factor becomes strengthened, the delay in the appearance of volume vaporization decreases.

Based on the experiments carried out, the process of formation of a laser erosion flame produced by the action of laser radiation of moderate intensity on metals can be represented as follows. For low power densities, the target material is only heated. As the power density increases, the melting of the metal in the irradiated zone and then vaporization occur. As this takes place, the erosion flame begins to form, and initially it consists of a transparent vapor and a plasma. These processes have been considered in [12] in detail. As the power density of the acting radiation increases further, volume vaporization appears and the finely dispersed liquid-drop phase begins to enter the erosion flame, initially, with a marked time delay. Then, as the intensity of irradiation increases, the delay decreases and becomes minimum. Liquid drops formed owing to volume vaporization, moving toward the laser beam, absorb and scatter it. Near the surface of the target, particles are crushed and vaporized completely as a consequence of superheating and form a denser plasma medium around themselves [1] as compared to that formed as a result of adiabatic expansion of the transparent vapor [12]. Such a medium causes a sharp, avalanche-like increase in the absorption coefficient of the plasma when the power density of the acting radiation reaches a certain value, and the plasma parameters (concentration of charged particles and temperature) increase sharply [1]. In this case, there occurs a plasma flash (plasma breakdown) in the erosion laser flame, which is initiated by completely vaporized particles of the liquid-drop phase of the target material. The case of plasma flash, where the radiation loss is determined by the mechanisms of absorption in the plasma, has been described theoretically in sufficient detail in [18–23].

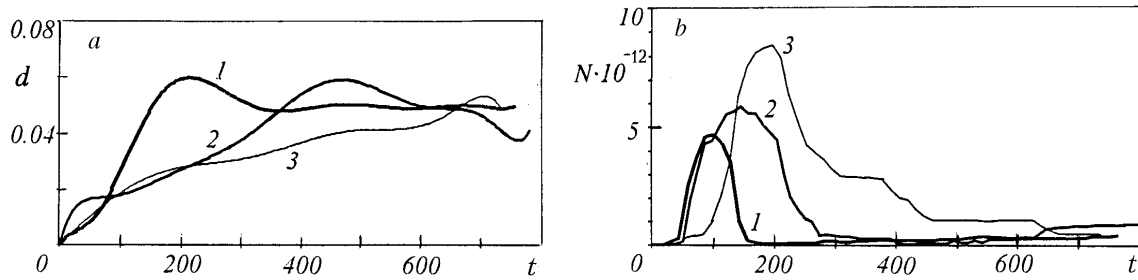


Fig. 10. Time variation of the diameters of particles (a) and their concentrations (b) in the erosion laser flame of the lead target for different values of the external electric field strength: 1) without an external field; 2) 1 kV/cm; 3) 4.  $t$ ,  $\mu\text{sec}$ ;  $d$ ,  $\mu\text{m}$ ;  $N$ ,  $\text{cm}^{-3}$ .

Thus, initially the erosion flame is practically transparent to radiation, and when a finely dispersed liquid-drop phase of the target material is formed in it, the loss of radiation in the laser-erosion products becomes marked. This loss is due to the absorption and scattering on liquid drops. After the plasma flash, the main radiation loss is determined by the absorption mechanisms in the plasma.

The efforts to obtain erosion plasma flows of metal targets, which would be free of drops, by increasing the power density of the acting radiation led to the fact that smaller particles began to enter the erosion flame; however, the concentration of particles increased.

In this connection, it is very important to find methods that would allow one to control the parameters of the liquid-drop phase of erosion laser flames of metals and to find methods of producing erosion flames free of drops.

In this regard the action of external electric and electromagnetic fields on the erosion laser flame can be promising.

In such experiments, the target was placed between two plates to which an external electric field perpendicular to the axis of the flame was applied. The action was performed by a rectangular pulse of the neodymium laser radiation with a power density of  $4.6 \cdot 10^5 \text{ W/cm}^2$ . The size and concentrations of liquid drops were monitored by the method of probing of the flame by the radiation of an auxiliary ruby laser. The probing was performed at a height of 1 mm from the target surface. The electric field was changed from 0 to 4 kV/cm.

Figure 10a shows the time variation of the diameter of particles in the erosion flame of the lead target. For a strength of the external electric field of 1 kV/cm, the curve of time variation of the diameter of the particles 2 reaches the maximum after 400  $\mu\text{sec}$ , while without an external electric field the maximum is observed at the 200th  $\mu\text{sec}$  (curve 1) after the beginning of the action. At a strength of 4 kV/cm, the maximum of curve 3 corresponds to a time of 700  $\mu\text{sec}$ . The number concentration of the particles increases with increase in the strength of the external electric field (Fig. 10b). It may also be suggested that as the strength of the external electric field increases further, the diameters of the liquid-drop-phase particles will decrease and the number concentration will increase. Such a time behavior of the parameters of the liquid-drop-phase particles can be explained by the spatial redistribution of electric charges on the surface of the particles, which stimulates their crushing [24, 25].

The investigations have shown that in the case where neodymium-laser radiation acts on a lead target exposed to the external electric field, the concentration of particles in the erosion laser flame is higher and the particle size is smaller as compared to the case where the action is performed without an electric field. This phenomenon can be used for control of the size and concentrations of particles in two-phase flows formed as a result of the action of laser radiation on metals.

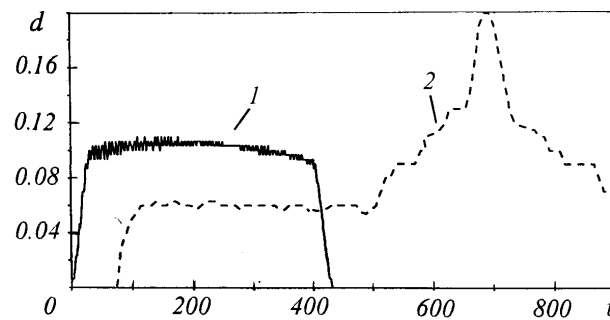


Fig. 11. Time behavior of the laser radiation intensity (1) (arbitrary units) and time variation of the size of liquid-drop-phase particles (2) in the erosion flame of the lead target.  $t$ ,  $\mu\text{sec}$ ;  $d$ ,  $\mu\text{m}$ .

We now consider the kinetics of particles of the condensed phase of the metal-target material in crossed laser beams when the acting laser radiation is directed perpendicularly to the surface of the target and the auxiliary laser radiation is directed parallel to the surface at a certain distance from it. The auxiliary laser radiation interacts with the erosion products without changing the conditions on the target surface [26].

As the acting radiation, we used nearly rectangular pulses of a neodymium laser with a 400–500- $\mu\text{sec}$  duration. In all the experiments, the power density of the acting radiation was  $1.4 \cdot 10^6 \text{ W/cm}^2$  for a diameter of the irradiated spot of 0.6 cm. As the completely vaporizing radiation, we used the radiation of a pulsed neodymium laser operating in the free-running mode. The pulse duration was  $\sim 10^{-3}$  sec and the diameter of the laser beam in the complete-vaporization zone was 0.8 cm. The axis of the completely vaporizing laser beam was positioned at a distance of 2 mm from the target surface. The investigations were carried out for different power densities of completely vaporizing radiation.

The general pattern of formation of the liquid-drop phase of the target material in the absence of completely vaporizing laser radiation is presented in Fig. 11.

It should be noted that the size of large particles is somewhat understated in our measurements, since, on the one hand, the procedure of monitoring of the particle size by the ratio between the scattered and the absorbed components of the probing ruby-laser radiation ( $\lambda = 0.7 \mu\text{m}$ ) is difficult to use for a lead target for a particle size of more than  $10 \mu\text{m}$ . In this case, monitoring of large particles was performed with a large error, because of the ambiguity of the ratio between the scattered and the absorbed components for some diameters and because of the weak dependence of the particle size on this ratio. On the other hand, because of the insignificant amount of very large particles in the erosion flame, the probability exists that they fly past the probing beam, whose diameter is 1 mm in our case. However, in the present work, most of the attention is concentrated on monitoring the size of particles that become smaller in the process of their complete vaporization. In this case, the use of the procedure proposed is quite justified.

The kinetics of the condensed phase in crossed laser beams can depend strongly on the particle size. Therefore, it makes sense to consider the cases where the following particles are present in the erosion flame: (1) small particles owing to volume vaporization (for the time of action of the plasma-forming pulse of a neodymium laser); (2) mainly large particles formed through the hydrodynamic mechanism (as is seen from Fig. 11, this occurs 650–700  $\mu\text{sec}$  after the beginning of laser action on the target); (3) particles formed through the two mechanisms (according to Fig. 11, this occurs 450–500  $\mu\text{sec}$  after the beginning of laser action).

The experiments have shown that complete vaporization of condensed-phase particles formed owing to volume vaporization begins for a power density of the completely vaporizing laser of  $\sim 10^5 \text{ W/cm}^2$ , while for  $\sim 5 \cdot 10^5 \text{ W/cm}^2$  particles become so small that the probing ruby-laser radiation scattered by them is beyond the sensitivity limits of the measuring system.

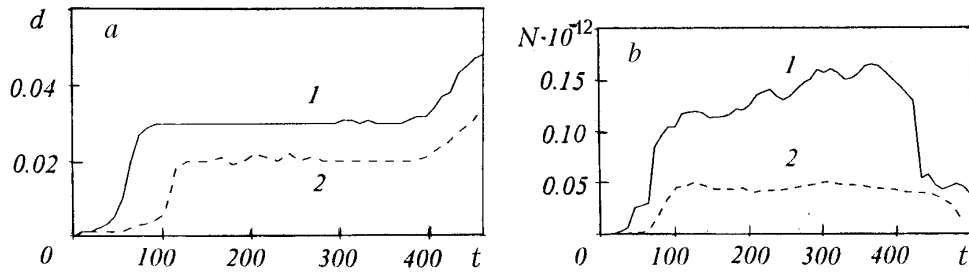


Fig. 12. Time variation of the diameters (a) and concentration (b) of particles of the liquid-drop phase of the lead erosion flame, which are formed due to volume vaporization: 1) without completely vaporizing laser radiation; 2) with this radiation.  $t$ ,  $\mu\text{sec}$ ;  $d$ ,  $\mu\text{sec}$ ;  $N$ ,  $\text{cm}^{-3}$ .

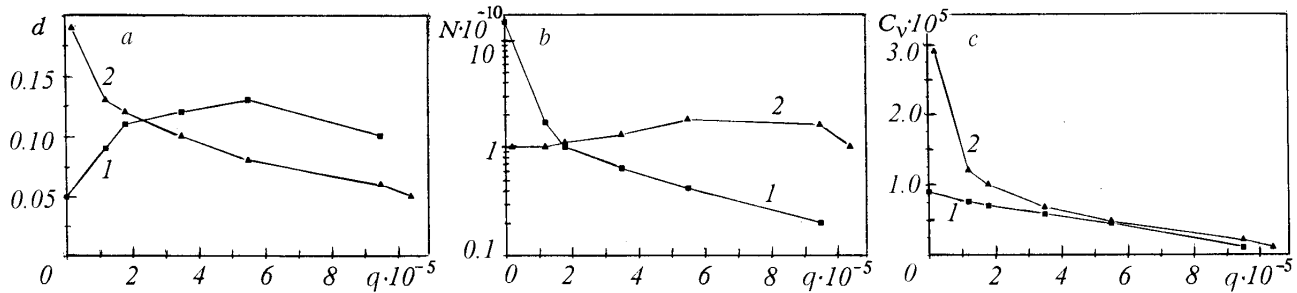


Fig. 13. Variation of the size (a) and the number (b) and volume concentrations (a) of particles of the liquid-drop phase of the erosion flame of the lead target with increase in the power density of the completely vaporizing laser. The moment of detection is 500 (1) and 700 (2)  $\mu\text{sec}$  after the beginning of the action.  $q$ ,  $\text{W}/\text{cm}^2$ ;  $d$ ,  $\mu\text{m}$ ;  $N$ ,  $\text{cm}^{-3}$ .

Figure 12 shows the results of experiments on the action of neodymium-laser radiation with a power density  $1.4 \cdot 10^6 \text{ W}/\text{cm}^2$  on a lead target in the absence of completely vaporizing laser radiation and in the presence of such radiation of power density  $q = 2.3 \cdot 10^5 \text{ W}/\text{cm}^2$ . It is seen that even for a low intensity of the completely vaporizing laser radiation (as compared to the acting radiation) the size of the condensed-phase particles and their concentration markedly decrease. For a higher power density of the completely vaporizing laser radiation, particles of the liquid-drop phase of erosion laser flames are no longer detected.

Figure 13 (curves 1) shows results of experiments for an instant of time of 500  $\mu\text{sec}$  after the beginning of the action of a radiation pulse of a neodymium laser on a target, when condensed-phase particles formed through the two mechanisms of formation are present in the erosion flame. In this case, the acting radiation also had a power density of  $q = 1.4 \cdot 10^6 \text{ W}/\text{cm}^2$ . The power density of the completely vaporizing radiation changed from 0 to  $\sim 10^6 \text{ W}/\text{cm}^2$ . The increase in the dependence  $d = f(q)$  to a certain maximum, which is shown in Fig. 13a (curve 1), can be explained by the fact that the smallest particles formed owing to the process of volume vaporization are completely vaporized and a larger fraction of large particles formed through the hydrodynamic mechanism remains in the flame. As the power density of the completely vaporizing radiation increases further, the size of the large particles decreases. The foregoing is well illustrated by Fig. 13b (1), where the behavior of the number concentration of particles as a function of the change in the power density is shown. The decrease in the volume concentration, which is shown in Fig. 13c (1), is evidence in favor of a fairly effective complete vaporization of the condensed phase of the target material for an increased power density of the completely vaporizing radiation. If the energy of the completely vaporizing laser increases further, the liquid-drop-phase particles are vaporized completely.

At an instant of time of 700  $\mu$ sec after the beginning of the action of laser radiation on the target, when fairly large particles formed through the hydrodynamic mechanism are present in the erosion flame, the particle size decreases with increase in the power density of the completely vaporizing radiation. However, in this case, the number concentration increases initially (see Fig. 13b (2)), which can be explained by the crushing of certain particles due to the superheating, and then, because of the competition of the processes of crushing of particles and their vaporization, complete vaporization becomes predominant and the number of particles decreases. The behavior of the volume concentration (see Fig. 13c (2)) points to the fact that the mass of the material contained in the particles of the condensed phase decreases significantly with increase in the power density of the completely vaporizing radiation, and particles can be vaporized completely for a certain power density.

Thus, investigations of the kinetics of particles of the condensed phase of erosion flames in crossed laser beams have shown that, using the action of auxiliary-laser radiation, one can exert efficient control of the parameters of the liquid-drop-phase particles and in so doing of the parameters of the erosion laser flames themselves. It is shown that to do this it is necessary that the power density of the completely vaporizing laser radiation be lower than the power density of the acting radiation and much lower for particles formed owing to volume vaporization. The power densities necessary for complete vaporization of particles formed through the hydrodynamic mechanism can also be decreased if an erosion laser flame is exposed to an external electric field: liquid-drop-phase particles crushed under the action of electric forces are easier to completely vaporize by auxiliary-laser radiation.

The results of the investigations carried out can be used to obtain controlled model two-phase flows in which it would be possible to change the parameters of the liquid-drop phase (diameters of the particles and their concentration) using an external electric field and an additional completely vaporizing laser radiation and to obtain a "sterile" erosion plasma free of drops, which is necessary in solution of a number of technical problems.

## REFERENCES

1. V. K. Goncharov, *Inzh.-Fiz. Zh.*, **66**, No. 5, 665–684 (1992).
2. V. S. Burakov and V. V. Zhukovskii, *Zh. Prikl. Spektrosk.*, **8**, No. 6, 943–948 (1968).
3. V. K. Goncharov, V. G. Kvachenok, A. V. Kolesnik, V. N. Kolesnikov, V. L. Kontsevoi, V. V. Revinskii, S. K. Tovmasyan, and A. F. Chernyavskii, *Optical Multichannel Analyzer for Studying Two-Dimensional Distributions of Intensity* [in Russian], Preprint No. 12 of the Physical Institute of the USSR Academy of Sciences, Moscow (1986).
4. V. K. Goncharov, V. L. Kontsevoi, M. V. Puzyrev, and A. S. Smetannikov, *Prib. Tekh. Éksp.*, No. 5, 145–155 (1995).
5. V. K. Goncharov and V. I. Karaban', *Zh. Prikl. Spektrosk.*, **45**, No. 1, 22–25 (1986).
6. A. P. Byk, V. K. Goncharov, V. V. Zakhozhii, V. G. Kvachenok, V. V. Revinskii, A. M. Starovoitov, and A. F. Chernyavskii, *Prib. Tekh. Éksp.*, No. 3, 244 (1987).
7. Yu. V. Afanas'ev and O. N. Krokhin, *Tr. FIAN — Kvantovaya Fizika* (Moscow), **52**, 118–170 (1970).
8. N. N. Rykalin and A. A. Uglov, *Fiz. Khim. Obrab. Mater.*, No. 2, 30–33 (1970).
9. V. B. Brekhovskikh, N. N. Rykalin, and A. A. Uglov, *Dokl. Akad. Nauk SSSR*, **190**, No. 5, 1059–1062 (1970).
10. B. M. Zhiryakov, N. N. Rykalin, A. A. Uglov, and A. K. Fannibo, *Kvantovaya Élektron.*, No. 1 (13), 119–121 (1973).
11. V. K. Goncharov, V. L. Kontsevoi, M. V. Puzyrev, and A. S. Smetannikov, *Inzh.-Fiz. Zh.*, **66**, No. 6, 662–667 (1994).

12. S. I. Anisimov, Ya. A. Imas, G. S. Romanov, and Yu. V. Khodyko, *Effect of High-Power Radiation on Metals* [in Russian], Moscow (1970).
13. A. M. Bonch-Bruevich, V. P. Kovalev, G. S. Romanov, Ya. A. Imas, and M. N. Libenson, *Zh. Tekh. Fiz.*, **38**, No. 4, 677–685 (1968).
14. A. G. Goloveiko, *Izv. Vyssh. Uchebn. Zaved., Énergetika*, No. 6, 667–685 (1966).
15. S. I. Anisimov, M. I. Tribel'skii, and Ya. G. Epel'baum, *Zh. Éksp. Teor. Fiz.*, **78**, No. 7, 1596–1605 (1980).
16. A. A. Samokhin, *Tr. IOFAN*, **13**, 3–107 (1988).
17. V. K. Goncharov, V. L. Kontsevoi, and M. V. Puzyrev, *Kvantovaya Élektron.*, **22**, No. 3, 249–252 (1995).
18. G. G. Vilenskaya and I. V. Nemchinov, *Prikl. Mekh. Tekh. Fiz.*, No. 6, 3–19 (1969).
19. G. G. Vilenskaya and I. V. Nemchinov, *Dokl. Akad. Nauk SSSR*, **186**, No. 5, 1048–1051 (1969).
20. G. G. Vilenskaya and I. V. Nemchinov, *Zh. Prikl. Spektrosk.*, **11**, No. 4, 637–643 (1969).
21. I. V. Nemchinov and S. P. Popov, *Pis'ma Zh. Éksp. Teor. Fiz.*, **11**, No. 9, 459–462 (1970).
22. I. V. Nemchinov and S. P. Popov, *Prikl. Mekh. Tekh. Fiz.*, No. 5, 35–45 (1971).
23. V. I. Bergel'son, A. P. Golub', T. V. Loseva, I. V. Nemchinov, T. I. Orlova, S. P. Popov, and V. V. Svetsov, *Kvantovaya Élektron.*, **1**, No. 5, 1268–1271 (1974).
24. V. E. Badan, V. V. Vladimirov, and V. Ya. Poritskii, *Zh. Tekh. Fiz.*, **57**, No. 6, 1197–1198 (1987).
25. V. E. Badan, V. V. Lisitchenko, and V. Ya. Poritskii, *Zh. Tekh. Fiz.*, **59**, No. 8, 141–142 (1989).
26. V. K. Goncharov and M. V. Puzyrev, *Kvantovaya Élektron.*, **24**, No. 4, 329–332 (1997).